Alzheimer-like Paired Helical Filaments and Antiparallel Dimers Formed from Microtubule-associated Protein Tau In Vitro

Holger Wille, Gerard Drewes, Jacek Biernat, Eva-Maria Mandelkow, and Eckhard Mandelkow

Max-Planck-Unit for Structural Molecular Biology, c/o DESY, D-2000 Hamburg 52, Germany

Abstract. Recent evidence from several laboratories shows that the paired helical filaments of Alzheimer's disease brains consist mainly of the protein tau in an abnormally phosphorylated form, but the mode of assembly is not understood. Here we use EM to study several constructs derived from human brain tau and expressed in *Escherichia coli*. All constructs or tau isoforms are rodlike molecules with a high tendency to dimerize in an antiparallel fashion, as shown by antibody labeling and chemical crosslinking. The length of the rods is largely determined by the region of internal repeats that is also responsible for microtubule binding. One unit length of the repeat domain (three or four repeats) is around 22–25 nm, comparable to the cross-section of Alzheimer PHF cores.

Constructs corresponding roughly to the repeat region of tau can form synthetic paired helical filaments resembling those from Alzheimer brain tissue. A similar self-assembly occurs with the chemically crosslinked dimers. In both cases there is no need for phosphorylation of the protein.

THE function of microtubules depends largely on their associated proteins (MAPs)[1] whose expression, distribution, and posttranslational modification is tissue specific and developmentally regulated (for review see Wiche et al., 1990; Tucker, 1990). Tau protein, a group of medium-sized MAPs, is prominent in neurons, particularly in axons, and one of its roles is thought to be the stabilization of microtubule arrays (Drubin and Kirschner, 1986). It has recently attracted attention because of its potential significance in Alzheimer's disease since tau is a main component of the Alzheimer-paired helical filaments (PHFs; for review see Kosik, 1990; Goedert et al., 1991). To understand tau's function in normal and pathological conditions it would therefore be necessary to investigate its structure and self-assembly.

The primary structure is known: tau is a mixture of isoforms arising from alternative splicing; in human brain there are six variants with 352–441 residues (Lee et al., 1988; Himmler et al., 1989; Goedert et al., 1988, 1989). Tau protein purified from brain has very little secondary structure (as judged by CD spectroscopy), and a sedimentation constant of 2.6 S, pointing to a highly asymmetric shape (Cleveland et al., 1977), in agreement with electron microscopic data (Hirokawa et al., 1988). The COOH-terminal half contains three or four internal repeats which are involved in microtubule binding and promoting their assembly (hence "assembly domain"). This domain can be phosphorylated by several protein kinases (Steiner et al., 1990; Drewes et al., 1992), a point that may be significant in view of the abnormal phosphorylation of Alzheimer tau (Grundke-Iqbal et al., 1986; Baudier and Cole, 1987; Biernat et al., 1992; Lichtenberg-Kraag et al., 1992). Moreover, the repeat region also lies in the core of Alzheimer-paired helical filaments (Goedert et al., 1988; Kondo et al., 1988; Ksiezak-Reding and Yen, 1991; Jakes et al., 1991).

These observations set the scene for the questions we want to answer: what is the shape and structure of the different tau isoforms? How do tau molecules associate with one another? In particular, is there a special interaction involving the repeat region which could explain the formation of paired helical filaments?

Previous work had already shown that tau has a tendency to self-associate into fibers (Montejo de Garcini and Avila, 1987; Lichtenberg-Kraag and Mandelkow, 1990). These studies were done with mixtures of tau from brain, and in mixed states of phosphorylation. We have now tried to circumvent the problem of heterogeneity by using recombinant tau expressed in *Escherichia coli*, as well as constructs obtained by directed mutagenesis. The results show that the length of tau is largely determined by the assembly domain, that the repeats form roughly a "unit" of length, and that monomers tend to dimerize in an antiparallel fashion. Tau constructs consisting only of the repeat region can form paired helical filaments in vitro, starting from both monomeric or dimeric subunits, and without being phosphorylated.

Correspondence should be addressed to E. Mandelkow.

1. *Abbreviations used in this paper*: CD, circular dichroism; FPLC, fast protein (peptide) liquid chromatography; MBS, m-maleimidobenzoyl-*N*-hydroxysuccinimide ester; MAP, microtubule-associated protein; NTP, nucleoside 5'-triphosphate; PCR, polymerase chain reaction; PDM, *N,N'*-p-phenylene-dimaleimide; PHF, paired helical filaments.

Materials and Methods

Cloning and Expression of Tau Constructs

Plasmid preparations and cloning procedures were performed according to Sambrook et al. (1989). PCR amplifications were carried out using Taq polymerase as specified by the manufacturer (Perkin Elmer Cetus, Hayward, CA) and a DNA TRIO-Thermoblock (Biometra, Göttingen, Germany).

Tau cDNA clones and their constructs were subcloned into the expression vector pNG2 (a derivative of pET-3b, Studier et al., 1990, modified in our laboratory by removal of PstI, HindIII, NheI, and EcoRV restriction sites for convenient engineering of the tau clones), or in expression vector pET-3a. For the expression we used the BL21 (DE3) *E. coli* system (Studier et al., 1990). All residue numbers refer to the sequence of htau40, the largest of the human isoforms (441 residues; Goedert et al., 1989). For the isolation of the constructs we made use of the heat stability of the protein; they were separated by fast protein (peptide) liquid chromatography (FPLC) Mono S chromatography (Pharmacia Fine Chemicals, Piscataway, NJ) (for details see Hagestedt et al., 1989).

Construction of T8R-1

This is a tau derivative containing eight repeats. It was constructed on the basis of the bovine tau4 isoform (Himmler et al., 1989). Two plasmids, pETNde43-12 (containing the btau4 gene) and pET-K0 (containing K0 which consists mainly of the four repeats plus leading and trailing sequences from the vector; Steiner et al., 1990) were used for the construction of T8R-1. The NdeI–RsaI DNA fragment from btau4 was connected with "filled in" XmaI–BamHI fragment of K0 leading to a chimeric molecule consisting of 553 amino acids. The T8R-1 gene encodes MetI-Val393 connected through the artificially introduced Ser residue with the Gly248–Tyr394 tau fragment, followed by a 23-residue tail from the bacteriophage T7 sequence (htau40 numbering).

Construction of T7R-2 and T8R-2

T7R-2 is a tau derivative containing seven repeats, T8R-2 contains eight repeats. Both molecules were constructed on the basis of the human htau23 and htau24 isoforms (Goedert et al., 1988). For the engineering of the T7R-2 and T8R-2 molecules, PCR repeat cassettes A1 (encoding four repeats), A2 (encoding the whole carboxy part of the tau24 molecule including the four repeat sequence and the tau sequence behind them) and A3 (encoding three repeats) were prepared. The T8R-2 molecule was generated by combination of A1 and A2 with NdeI–PstI DNA fragment isolated from htau24. This tau derivative consists of 511 amino acids, the first 311 NH_2-terminal residues of htau24 (MetI-Lys369, containing four repeats), followed by Gly–Thr link, then by 198 residues of the COOH terminus of htau24 (Gln244-Leu441, four more repeats). The T7R-2 gene was generated similarly to T8R-2 but the A3 cassette was used instead of A1. The T7R-2 protein consists of 480 amino acids, the first 280 NH_2-terminal residues of htau23 (MetI-Lys369, including three repeats), followed by Gly–Thr link, then by 198 residues of the carboxy-terminal part of htau24 (Gln244-Leu441, containing four repeats, htau40 numbering).

Construction of K11 and K12

They were constructed by combination of fragments derived from the htau23 and htau24 genes. K11 is a tau derivative containing four repeats and consists of 152 amino acids (Q244-Y394 plus start methionine). K12 is a tau derivative containing three repeats and consists of 121 amino acids (Q244-Y394 plus start methionine, but without the second repeat V275-S305, htau40 numbering).

Chemical Cross-linking

Construct K12 (2–5 mg/ml) in 40 mM Hepes, pH 7.5, was incubated with 0.5 mM DTT for 30 min at 37°C and then reacted for 30 min at room temperature with 0.7 mM PDM (Sigma Chemical Co., St. Louis, MO) or 1.5 mM MBS (Pierce Chemical Co., Rockford, IL) added from freshly prepared stock solutions in DMSO. The reactions were quenched by addition with 5 mM DTT or 5 mM DTT and 5 mM ethanolamine, respectively.

Gel Filtration

The covalently cross-linked dimers were separated from the monomers by gel filtration on a Superose 12 FPLC column (Pharmacia Fine Chemicals) equilibrated and eluted with 50 mM Tris-HCl, pH 7.6, containing 0.5 M NaSCN, 0.5 M LiCl, and 2 mM DTT operated at a flow rate of 0.3 ml/min. Column fractions were analyzed by SDS-PAGE, pooled, and concentrated by centrifugation through centricon 3 microconcentrators (Amicon Corp., Danvers, MA). The column was calibrated with the proteins from the low molecular weight gel filtration calibration kit (Pharmacia Fine Chemicals). Effective hydrated Stokes radii (r) of the calibration proteins were taken from the kit's instruction manual and partition coefficients (σ) were determined from the elution volumes and fitted to an equation of the form $\sigma = -A \log r + B$, yielding the Stokes radii for the tau construct monomers and dimers. The axial ratios were calculated following Perrin (for methods see Cantor and Schimmel, 1980).

Glycerol Spray Experiments

Spraying was done following Tyler and Branton (1980). The samples were diluted 1:10 in spraying buffer (50 mM ammonium acetate, pH 8.0, 150 mM NaCl, 1 mM $MgCl_2$, 0.1 mM EGTA), made up to 70% glycerol and sprayed onto freshly cleaved mica. The sprayed samples were vacuum dried for 2 h, shadowed with platinum/carbon (~1.5 nm thick, shadowing angle 4°) using a BAE 080T shadowing unit (Balzers Union, Balzers, Liechtenstein), followed by 20–30 nm carbon. Finally the replicas were floated off on doubly distilled water and picked up with 600-mesh copper grids.

Antibody Labeling

Samples were mixed with a roughly fivefold excess of antibody (Map 2–4, kindly provided by Drs. J. Dingus and R. Vallee, Worcester Foundation, Shrewsbury, MA) (see Dingus et al., 1991) and incubated for 1–1.5 h at room temperature. Afterwards the samples were diluted 1:10 in spraying buffer and treated following the normal glycerol spray procedure.

Formation of Synthetic PHFs

Solutions of tau constructs or chemically cross-linked dimers were dialyzed against various buffers (e.g., ~50–500 mM MES, Tris-HCl, Tris-maleate, pH values 5–9, 5–30 mM $MgCl_2$, $CaCl_2$, $AlCl_3$) for 12–24 h at 4°C. The solution was briefly centrifuged (Heraeus Biofuge A, 1 min, 10,000 *g*). The pellet was stored for several days at 4°C and then processed for negative stain EM (2% uranyl acetate or 1% phosphotungstic acid). Alternatively the solution was used for grid dialysis on gold grids following Van Bruggen et al. (1986). PHFs were observed only in certain conditions and with certain tau constructs (pH 5–5.5, K11 or K12 and K12 dimers, see Results).

Electron Microscopy

The specimens were examined on a Philips CM12 microscope (Philips Electronic Instruments, Inc., Mahwah, NJ) at 35–60,000 magnification. Electron micrographs were taken on electron image film SO-163 (Eastman Kodak Co., Rochester, NY). Magnification calibration was performed using negatively stained catalase crystals.

Miscellaneous Procedures

SDS-PAGE was done following Laemmli (1970), with a gradient of 4–20%. Analytical ultracentrifugation (model E; Beckman Instruments Inc., Palo Alto, CA) and CD spectroscopy (Jobin-Yvon Dichrograph R. J. Mark III Instruments S.A., Munich, Germany) was kindly made available by Drs. A. Pingoud and C. Urbanke, Hannover.

Results

Conformation and Dimerization of Tau Constructs

Fig. 1 illustrates the types of constructs used in this study. We started out with the isoforms occurring in human brain, ranging from htau23 (the smallest isoform, 352 residues) to htau40 (the largest, 441 residues; see Goedert et al., 1989). They differ mainly by the number of internal repeats in the COOH-terminal domain (three or four) and the number of inserts near the NH_2 terminus (zero, one, or two). The internal repeats are involved in microtubule binding and in the formation of paired helical filaments. We therefore focused our attention on those constructs which would presumably

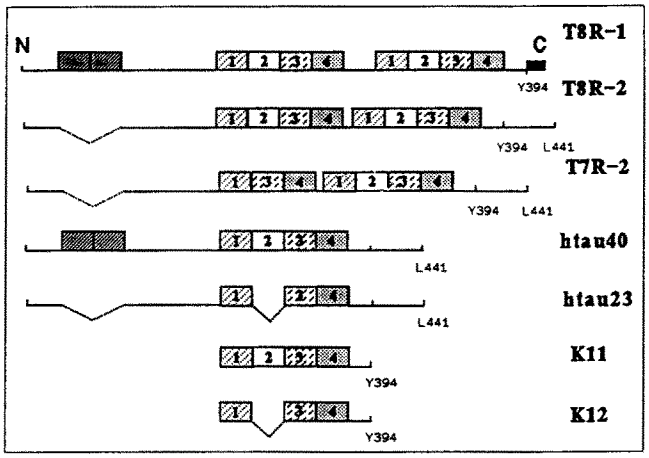

Figure 1. Diagram of tau isoforms and constructs used in this study. (*T8R-1*) 553 residues, molecular weight 57,743. It has two inserts near the NH_2-terminus (29 residues each, *hatched*), a repeat domain of four repeats (numbered 1–4) which is duplicated with a small spacer in between. (*T8R-2*) 511 residues, molecular weight 53,459; it lacks the NH_2-terminal inserts, but has the four repeats duplicated without spacer. (*T7R-2*) 480 residues, molecular weight 50,212; similar to T8R-2, but without the second repeat sequence in the first repeat domain. (*Htau40*) 441 residues, molecular weight 45,850 (Goedert et al., 1989), with two NH_2-terminal inserts and a repeat domain containing four repeats. (*Htau23*) 352 residues, molecular weight 36,760, the smallest of the human tau isoforms, without the NH_2-terminal repeats and only three repeats. (*K11*) 152 residues, molecular weight 16,326 a repeat domain with four repeats plus a short tail. (*K12*) 121 residues, molecular weight 13,079, a repeat domain with three repeats plus a short tail.

yield information on the structure of the repeat region. We used three types of molecules, (*a*) tau isoforms occurring in brain, such as htau23 or htau40, (*b*) engineered constructs with an increased number of repeats, e.g., seven or eight (T7, T8), and (*c*) constructs containing essentially the repeats only (e.g., K11, K12).

The SDS gels of Fig. 2 illustrate some of these proteins. Most tau constructs have relative molecular weights larger than expected from their actual mass (Fig. 2 *a*). A notable feature is the tendency to form dimers and oligomers. This is particularly pronounced with some constructs, for example K12 (Fig. 2 *b*). The formation of dimers can already be observed by letting the protein stand for some time (Fig. 2 *b*, lane *2*), presumably because the dimers become fixed by a disulfide bridge; this can be prevented by DTT (lane *1*). To test this, we used the cross-linker PDM which predominantly links cysteines. This generates essentially the same products as in the absence of DTT (lane *3*). Finally, dimers and higher oligomers can also be generated by MBS which links cysteines and lysines (lane *4*). The cross-linked species can be separated by chromatography on a Superose 12 column (Fig. 2 *c*), allowing us to study a homogeneous population of dimers. The elution profile (Fig. 2 *d*) yields Stokes radii of 2.5 nm for the monomer of K12, and 3.0 nm for the dimer. Given the molecular weights of 13 and 26 kD this yields axial ratios of 10 and 8, consistent with the rod-like shape observed by EM (the equivalent lengths of prolate ellipsoids would be 6.8 and 8.5 nm which underestimates the actual lengths, see below).

Other tau species show similar crosslinking results, but they are somewhat more complex for the following reason: tau has cysteines only in repeats 2 and 3 (residues Cys291 and Cys322). Repeat 2 is absent from some isoforms, for example htau23 or construct K12, leaving only the lone Cys322. With Cys–Cys cross-linkers such as PDM, these molecules can only form dimers, but no higher aggregates (Fig. 2 *b*, lane *3*). By contrast, bivalent molecules with two cysteines (such as htau40, K11) can form intramolecular cross-links, dimers, and higher oligomers. This diversity is similar to what we find after cross-linking of K12 with MBS (Fig. 2 *b*, lane *4*) because tau contains many lysines.

The conformation of several tau constructs in solution was probed by analytical ultracentrifugation and CD spectroscopy. For example, htau40 had a sedimentation constant of 2.6 S, similar to the results of Cleveland et al. (1977) on the mixture of tau from brain. For a globular particle of the mass of htau40 (45.8 kD) one would expect ~4.2 S; the lower observed value indicates an elongated structure with a hydrodynamic axial ratio of ~15. The CD spectra of htau40 and construct K12 (Fig. 2 *e*) were indistinguishable; they showed very little secondary structure, again in agreement with Cleveland et al. (1977). This means that both the NH_2-terminal and COOH-terminal domains of tau lack internal regularity such as α-helix or β-sheet.

Synthetic Paired Helical Filaments

Tau isolated from brain tissue can self assemble into fibrous structures, observed by several authors (e.g., Montejo de Garcini and Avila, 1987; Lichtenberg-Kraag and Mandelkow, 1990). This property became particularly interesting in view of the fact that tau is one of the main components of the neurofibrillary tangles of Alzheimer's disease. In the earlier studies the relationship of the filaments formed in vitro to the Alzheimer PHFs remained ambiguous, especially since the protein was heterogeneous. We therefore wanted to check if recombinant tau constructs were capable of self-assembly. This was tested in a variety of conditions of pH, salt, buffer type, etc. Of the constructs tested only K11 and K12 yielded filaments resembling PHFs. The optimal conditions were 0.3–0.5 M Tris-HCl and pH 5.0–5.5, and no other salts added. The results obtained with construct K12 are illustrated in Fig. 3. In the pH range of 5.0–5.5 there was extensive formation of filaments. Their length was variable, but typically in the range 200–1,000 nm. Most appeared rather smooth, others showed a regular variation of width, with axial periodicities around 70–75 nm (*arrowheads*). The minimum diameter was about 8 nm and the maximum around 15 nm. We also observed short rodlike particles, ~80–150-nm long, which appeared to represent just one or two crossover periods of the filaments (Fig. 3 *c*, middle). It was not possible to discern reliably any axial fine structure that might indicate an arrangement of protein subunits. This was therefore either below the resolution limit of negative stain, and/or due to lack of contrast. In general the filaments tended to be bundled up in clusters, as if they had a high affinity for one another (Fig. 3 *a*). Similar PHF-like filaments were also obtained with K12 dimers cross-linked with PDM (Fig. 4). This suggests that the dimer might be an intermediate stage in filament assembly.

Many of these features are similar to those of paired helical filaments isolated from Alzheimer disease brains, shown for

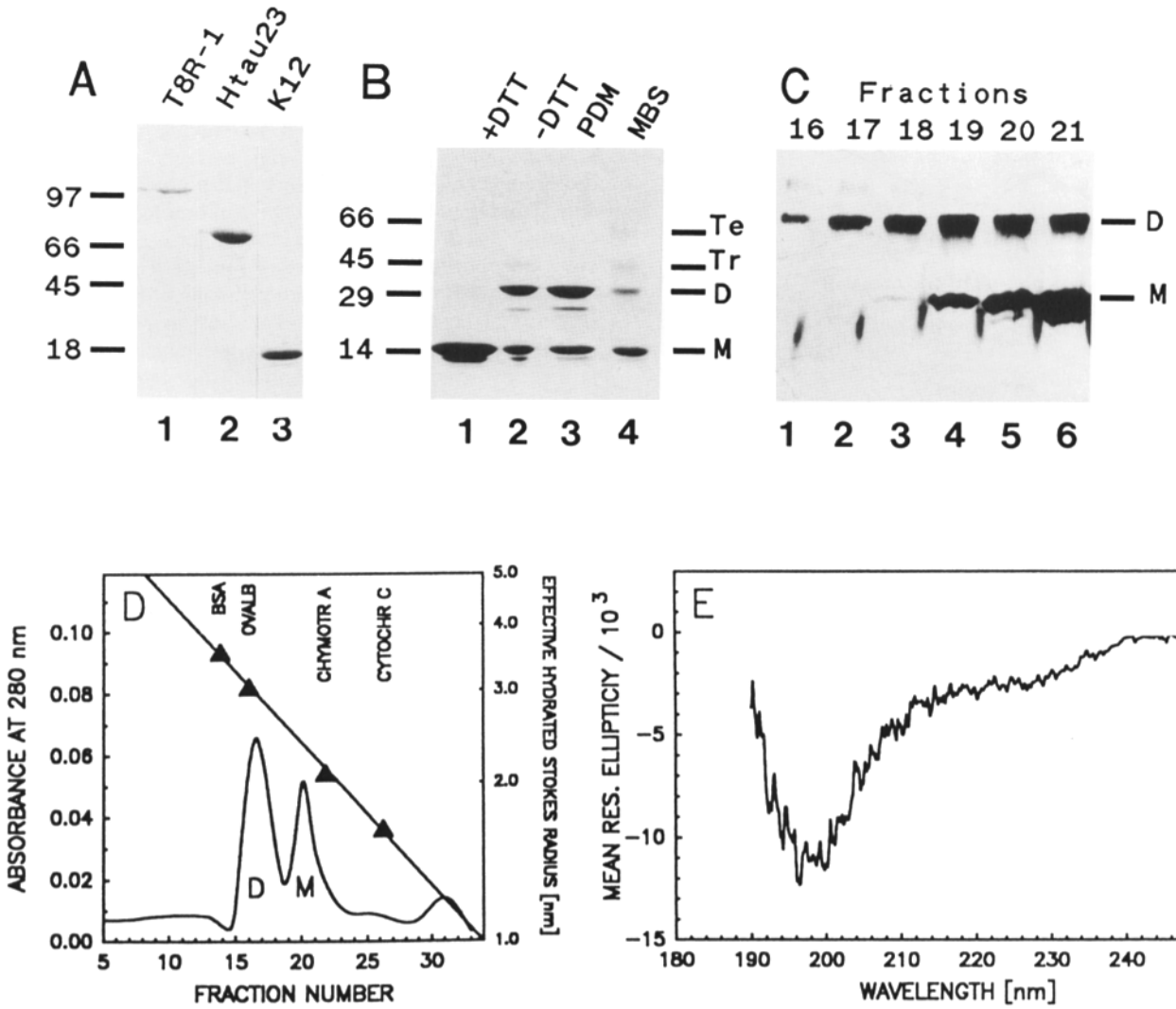

Figure 2. SDS-PAGE (4–20%) and gel chromatography of tau constructs and crosslinked products. *A* and *C* were run in reducing conditions (3 mM DTT in sample buffer), *B* in non-reducing conditions (except lane *1* with 3 mM DTT in sample buffer). (*A*) Constructs T8R-1, Htau23 and K12. Molecular weight markers are given on the left. (*B*) Construct K12 and crosslinked products. Crosslinking occurs spontaneously in the absence of DTT, it can be prevented by DTT, or induced by addition of PDM or MBS. Aggregation products are labeled on the right (monomers, dimers, trimers, tetramers, etc.). (*C*) Silver stained SDS gel of a Superose 12 gel filtration run of K12 cross-linked by PDM. The dimers (top band) elute before the monomers. Fractions 16 and 17 were used for EM. (*D*) Elution profile of Superose 12 gel filtration of construct K12 monomers and dimers cross-linked with PDM. The elution positions of calibration proteins are plotted against their effective hydrated Stokes radii on a logarithmic scale (right axis). (*E*) CD spectrum of construct K12 (8 mg/ml in 40 mM Hepes, pH 7.2, path length 0.01 mm). There is no significant α-helical or β-sheet structure. Simlar spectra are obtained with other constructs as well as with full length tau.

comparison in Fig. 5 (cf. Crowther and Wischik, 1985). Their appearance depends somewhat on the isolation procedure. Fig. 5 *a* shows "insoluble" filaments prepared from neurofibrillary tangles after Wischik et al. (1985). These filaments are long, straight, and have a homogeneous ultrastructure characterized by the distinct ~75-nm repeat. By contrast, when the filaments are "solubilized" by sarkosyl following Greenberg and Davies (1990) they are shorter and less homogeneous (Fig. 5 *b*). In particular this preparation includes very short particles (equivalent to about one to two crossover periods), and smooth filaments that do not have the twisted appearance (reminiscent of straight filaments, see Crowther, 1991; Goedert et al., 1992). There is a striking similarity between the synthetic PHFs based on the repeat domain (e.g., K11, K12, K12 dimers, Figs. 3 and 4) with the soluble PHFs from Alzheimer brains (Fig. 5 *b*), judged by three different criteria: (*a*) The filaments are shorter than the insoluble PHFs of Fig. 5 *a*; (*b*) they are less homogeneous in their periodicity, and some lack the twisted appearance altogether (straight filaments); and (*c*) they include very short rodlike particles, down to the length of one crossover period.

Thus far we have observed synthetic PHF-like fibers only with constructs such as K12 and K11 containing essentially the repeat domain (three or four repeats, Fig. 1), but not with larger tau isoforms. These data are all consistent with the assumption that the repeat domain is the basic unit that is capable of self-assembling into PHFs very similar to those of Alzheimer neurofibrillary tangles. This also agrees with

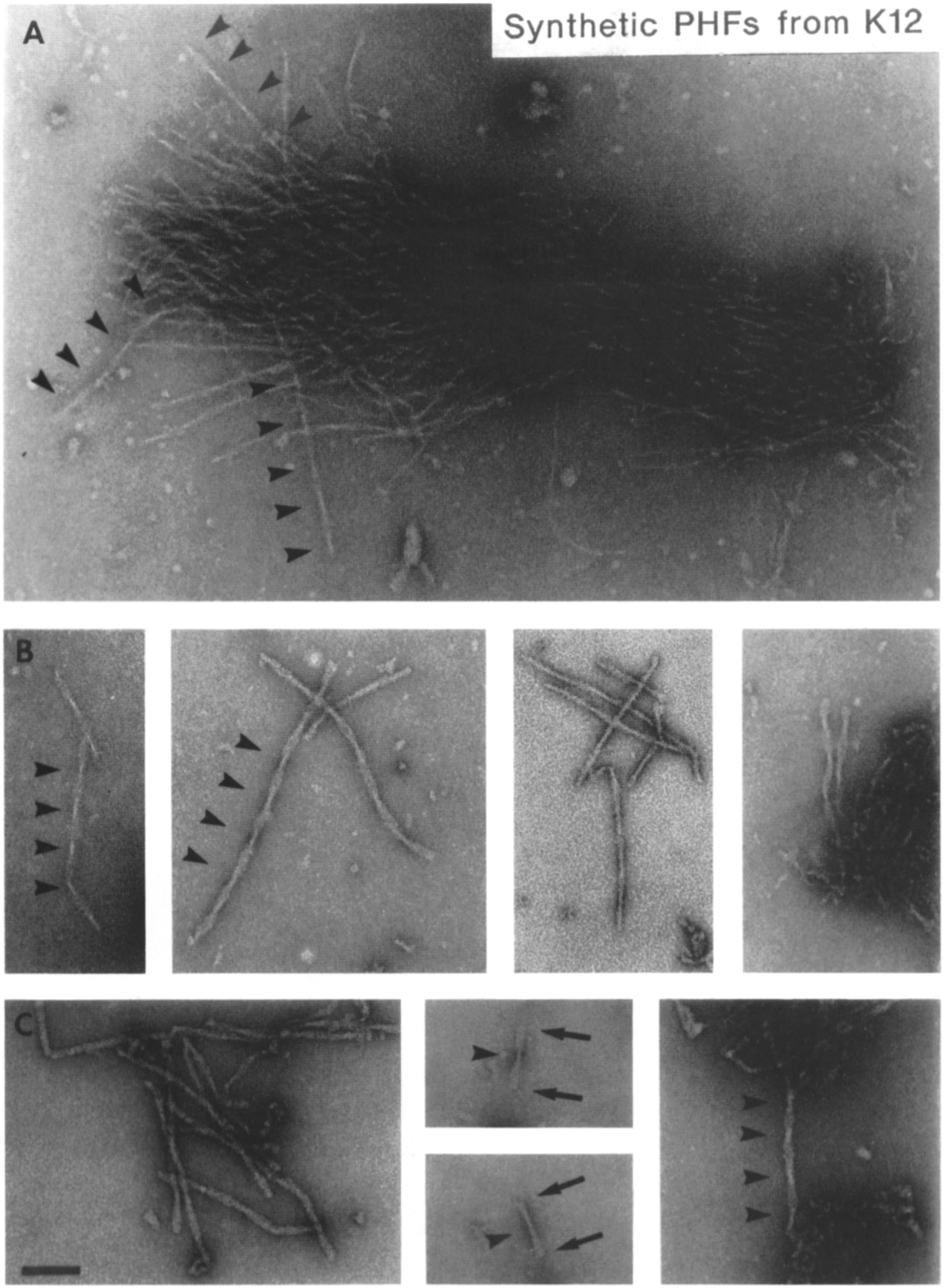

Figure 3. Synthetic paired helical filaments from construct K12. (*A*) A tangle of synthetic PHFs from K12 (crossover period of ≈70–75 nm indicated by *arrowheads*). The construct was expressed and purified by the methods described previously (Steiner et al., 1990). It was dialyzed against 0.5 M Tris-HCl, with pH values between 5.0 and 5.5. The solution was negatively stained with 2% uranyl acetate. (*B* and *C*) Single fibers of synthetic paired helical filaments made from construct K12. Note the crossover repeats (*arrowheads*) and the rodlike particles of lengths ~100 nm (*C, middle*). Bar, 100 nm.

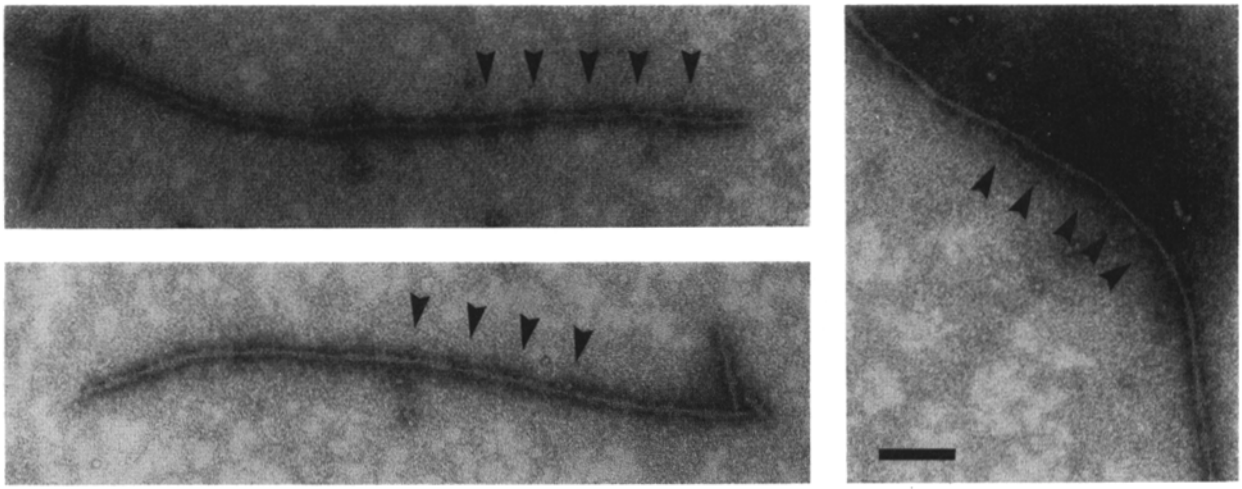

Figure 4. Synthetic paired helical filaments from K12 dimers crosslinked with PDM and negatively stained with 1% phosphotungstic acid (micrographs provided by M. Kniel, Max-Planck-Unit, Hamburg, Germany). Bar, 100 nm.

experiments in several laboratories showing that the pronase-resistant core of Alzheimer PHFs contains the repeat region (Goedert et al., 1988; Kondo et al., 1988; Ksiezak-Reding and Yen, 1991; Jakes et al., 1991). We also note that the filament-forming constructs were not phosphorylated so that this does not play a role in self-assembly here (in contrast to the genuine Alzheimer PHFs, see Discussion).

Electron Microscopy of Tau Monomers and Dimers

The results on the synthetic PHFs suggested that the repeat region had a special role in the interaction between tau molecules. We therefore tried to define their structure in more detail by comparing different constructs in the electron microscope. The method of choice is metal shadowing at a very shallow angle, combined with glycerol spraying; this helps to make the particles visible which otherwise would not be seen because of their low contrast.

Molecules of htau23 (352 residues, Fig. 6 *a*) are rodlike and have a mean length of 35 ± 7 nm (lengths summarized in Table I and Fig. 7). This value is less than that reported

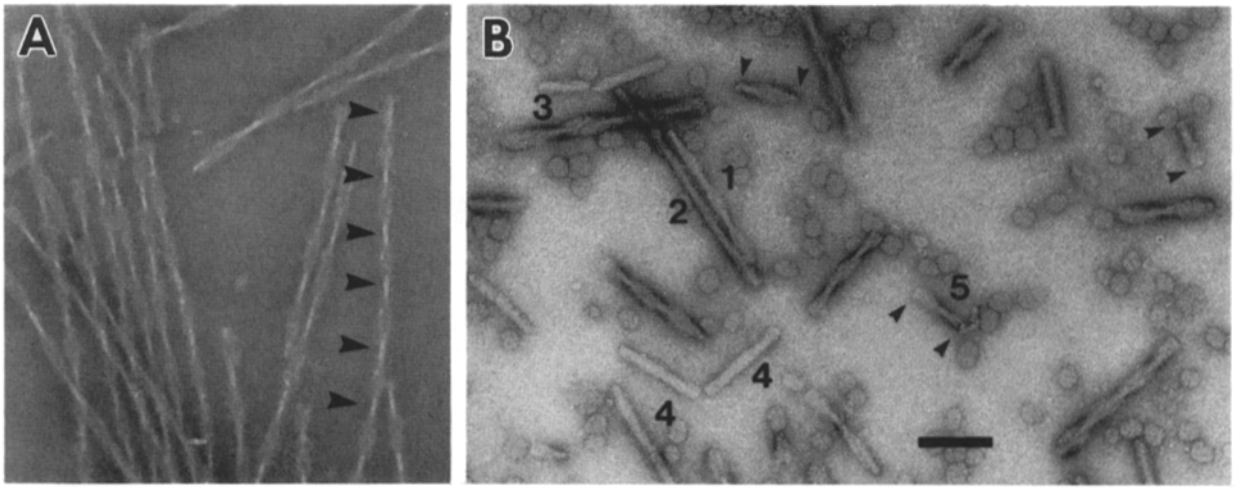

Figure 5. Paired helical filaments from Alzheimer brain (micrographs provided by Dr. Lichtenberg-Kraag, Max-Planck-Unit). (*A*) PHFs from neurofibrillary tangles prepared after Wischik et al. (1985), stained with 1% phosphotungistic acid. This preparation contains homogeneous long filaments which still retain their pronase sensitive "fuzzy coat." The cross-over repeat is 75–80 nm, the width varies between a minimum of ~10 nm and a maximum of 22 nm. (*B*) PHFs prepared after Greenberg and Davies (1990). This preparation results in soluble filaments of shorter length than in *A* and is more heterogeneous. (*1*) Paired helical filament with a 72-nm repeat and a width varying between 8 and 18 nm; (*2*) straight filament of 8-nm width; (*3*) twisted filament with a particularly wide diameter (up to 25 nm); (*4*) straight filament with a wide diameter (18 nm); (*5*) twisted rodlike particle ~80-nm long, equivalent to about one cross-over period. In many cases the particles appear to have broken apart across the filament, e.g., the two rods labeled 4, the twisted filament of *3* and the short stub to the right of it, or the two straight rods above particle (*3*). Bar, 100 nm.

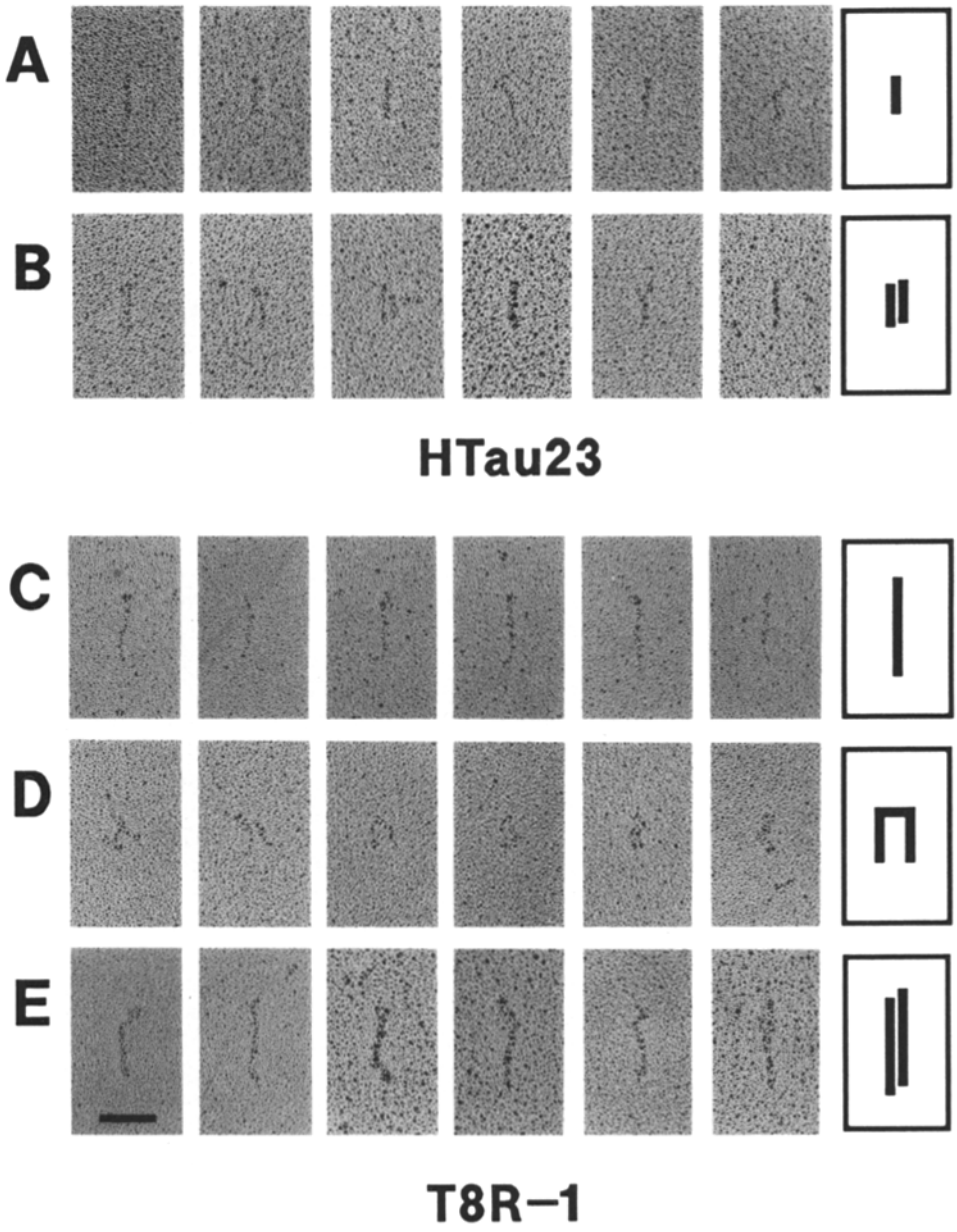

Figure 6. Electron micrographs of tau isoform htau23 and construct T8R-1 prepared by glycerol spraying and metal shadowing. (*a*) Monomers of htau23, (*b*) dimers of htau23, (*c*) monomers of T8R-1, (*d*) folded forms of T8R-1 (hairpin folds showing intramolecular antiparallel association), and (*e*) dimers of T8R-1. For lengths see Table I and Fig. 7. Interpretative diagrams are shown on the right. Bar, 50 nm.

by Hirokawa et al. (1988), but this might be due to differences in the experimental approach (freezing vs. glycerol spraying; a mixture of all isoforms vs. the smallest isoform). The apparent width of the metal shadowed htau23 molecules is about 3–5 nm, and the contrast is low—much less than that of control samples (single and double stranded DNA, α-helical proteins; for details see Wille et al., 1992*a*). Careful inspection of the micrographs reveals a population of particles with enhanced contrast, somewhat larger diameter (5–7 nm), sometimes split into two parts, and lengths similar to or slightly more than the monomer (around 40 nm). These particles are interpreted as (nearly) juxtaposed monomers forming dimers (Fig. 6 *b*), consistent with the results on cross-linked dimers and antibody decoration shown later.

Clearly longer particles are obtained with the construct T8R-1 which average 58 ± 15 nm, 23 nm more than htau23 (Figs. 6 *c*, and 7, *a* and *b*). This construct contains eight repeats (a duplication of the four basic ones, Fig. 1), that is five repeats more than htau23, plus the two 29-mer inserts near the NH_2 terminus. T8R-2 has a similar length (61 ± 17 nm), even though it lacks the NH_2-terminal inserts (not shown). Construct T7R-2 also has a similar length of 60 ± 16 nm, even though it has only seven repeats (3 + 4) and no NH_2-terminal inserts. At first sight these results appear puzzling: On the one hand, larger constructs become longer, but on the other hand certain parts of the sequence do not affect the length. Anticipating the results below, the contradiction can be explained by a unifying hypothesis: The length of the tau constructs is determined mainly by the repeat region; by comparison, the NH_2-terminal domain and the COOH-terminal tail are only of minor influence. The repeat region itself must be considered as a unit, roughly 20–25-nm long, whose length is approximately independent of the second repeat. The hypothesis implies that the N-terminal inserts have only a minor influence on the length. It predicts that constructs with three or four repeats have

Table I. Summary of Lengths of Various Tau Constructs

Construct	Length	SD	Number
	(*nm*)	(*nm*)	
htau23	35	7	232
T8R-1	58	15	304
T8R-2	61	17	75
T7R-2	60	16	73
K11	26	5	32
K11 dimer	32	6	24
K12	25	4	27
K12 dimer	30	4	25
K12 PDM dimer	29	6	79
K12 MBS dimer	34	6	85

roughly the same length (see T7R vs. T8R, or examples below), and that the addition of one repeat domain adds ~20–25-nm to the length (as in htau23 vs. T7R or T8R).

T8R and other constructs also form particles folded into a hairpin (Fig. 6 *d*), as if the two "units" (of four repeats each in this case) could interact; this is suggestive of an antiparallel arrangement, supporting the antibody data described later. We also observe T8R particles whose width and contrast indicate dimers, similar to htau23 (Fig. 6 *e*).

We now turn to K11 and K12, the repeat domain constructs that form the PHF-like fibers described above (Fig. 8). As in the previous cases the particles are rodlike. Using the criteria of thickness or contrast and the comparison with the dimers, we find for K11 a population of low contrast monomers with a mean length of 26 ± 5 nm (Fig. 8 *a*), and a population of more contrasty dimers, about 32 ± 6 nm (Fig. 8 *b*). This means that the two molecules must be juxtaposed for most of their length. For K12 we find monomers of length 25 ± 4 nm, (Fig. 8 *d*), and dimers of about 30 ± 4 nm (Fig. 8 *e*). Note that the monomers have ~70–75% of the length of htau23, although they contain only a third of the residues (Fig. 7, *c* and *e*). With both constructs we find longer particles which we interpret as dimers associated into tetramers (Fig. 8, *c* and *f*).

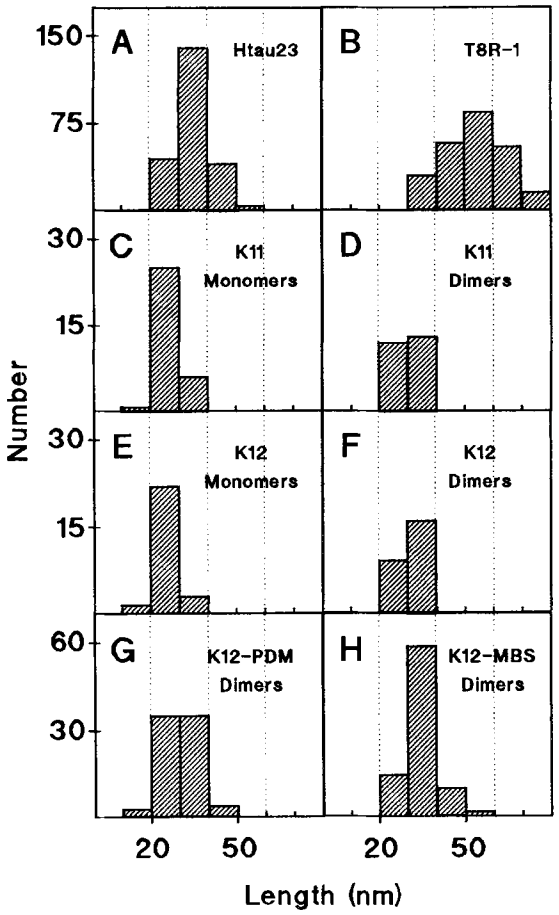

Figure 7. Length histograms of tau constructs and dimers.

Thus far the classification into monomers and dimers was judged by relating the width and contrast of the particles to model structures. However, it is possible to isolate the covalently cross-linked dimers by gel chromatography and study them directly by EM and other methods. As an example we show dimers of K12 cross-linked by PDM via the single Cys322 (Fig. 9 *a*). In the electron microscope their contrast is similar to the dimers described above; but more importantly, they are only slightly longer than the monomers (29 ± 6 nm, Figs. 9 *a*, and 7, *e* and *g*). This means that the PDM dimers are formed by two molecules lying next to one another and nearly in register. The dimers of K12 induced by MBS (34 ± 6 nm) are also similar, except that they tend to be somewhat longer (by ~5 nm) than those obtained with PDM, probably because a greater variety of Cys–Lys bonds are possible (Figs. 9 *b* and 7 *h*).

Taken together, the results obtained with K11 and K12 (and other constructs containing essentially the repeat domain) are consistent with the hypothesis that the repeat domain forms a folding unit of rather uniform length, independently of whether it contains three or four repeats.

Finally we note that for all constructs tested the glycerol spray experiments show a certain tendency to form fibrous structures. In most cases they are rather uniform in diameter, they show no obvious relationship to paired helical filaments and may result from a distinct pathway of self-assembly. These fibers will not be dealt with here, but examples have been shown previously for tau by Lichtenberg-Kraag and Mandelkow (1990) and similar ones for MAP2 by Wille et al. (1992*a*,*b*).

Antiparallel Alignment of Dimers

It is clear from the above data that tau and its constructs tend to align laterally into dimers. This raised the question of polarity: are the particles parallel or antiparallel? First indications came from the hairpin fold observed with the 8-repeat constructs (e.g., Fig. 6 *d*), suggesting antiparallel orientations of the two halves. Direct evidence for this was obtained by labeling with the mAb 2-4 whose epitope is on the last repeat and therefore close to the COOH terminus in terms of the sequence (Dingus et al., 1991). Fig. 10 a (*left*) shows particles of htau23 with one antibody molecule bound. The antibodies bind at or near one end, showing that one of the physical ends of the rod coincides roughly with the COOH terminus. The lengths of the rod portions shown are similar to that of unlabeled htau23; in terms of apparent width they could be monomers or dimers. In the same fields one also finds doubly labeled particles (Fig. 10 *a*, *right*). The antibodies bind at opposite ends, proving that the two subunits of a dimer have opposite polarities.

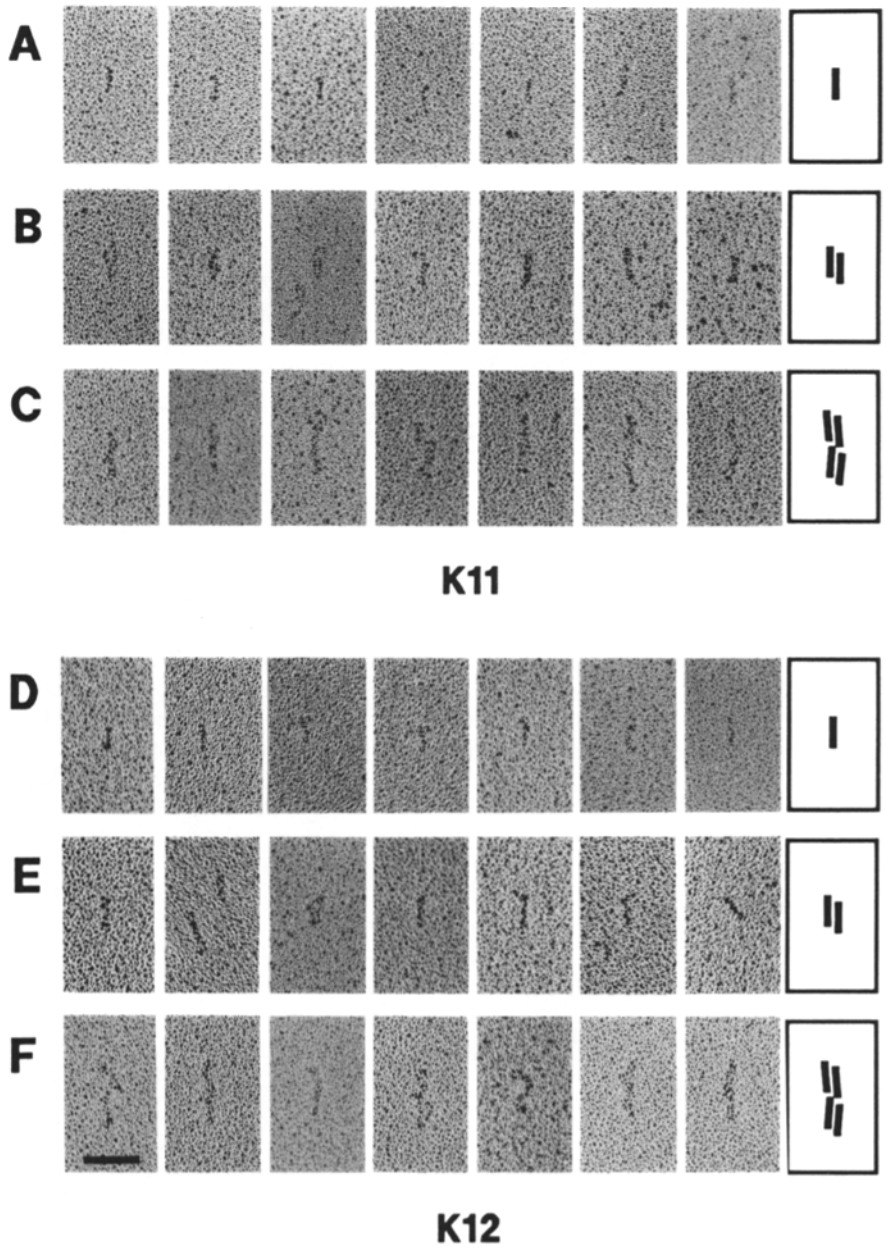

Figure 8. Electron micrographs of constructs K11 and K12. (*A*) Monomers of K11. (*B*) dimers of K11. (*C*) tetramers of K11 formed by longitudinal association of two dimers. (*D*) Monomers of K12, (*E*) dimers of K12. and (*F*) tetramers of K12. Bar, 50 nm.

The same features are found with construct K12: rodlike stubs with an antibody at one end (Fig. 10 *b*, *left*); dumbbells, i.e., antiparallel dimers (Fig. 10 *b*, *middle*). Finally, there are particles with two antibodies and two stubs, with a kink in the middle (pairs of "cherries," Fig. 10 *b*, *right*). Each of the arms has roughly the length of a unit stub so that the particles appear equivalent to the tetramers of Fig. 8 *c* and *f*. The interaction between the dimers at the center appears to prevent the binding of an antibody which could otherwise be expected there.

PDM dimers of construct K12 (formed by Cys322-Cys322 cross-links) are shown in Fig. 10 *c*. Particles with one antibody label are on the left, doubly labeled ones in the middle, showing that the chemically cross-linked dimer consists of antiparallel monomer. A presumptive tetramer is on the right. Essentially the same data are obtained with MBS cross-linked dimers (Cys322 to nearby Lys, Fig. 10 *d*).

Discussion

The Structure of Tau Monomers and Dimers

Our aim is to understand the structure of the MAP tau, the relationship between tau structure and microtubule-binding properties, and the self-assembly of tau that occurs in Alzheimer-paired helical filaments. Before discussing specific results it is useful to summarize a few general aspects. The sequence of all tau isoforms is rather hydrophilic, with little predicted secondary structure, as noted by Lee et al. (1988). This is consistent with the CD spectrum of tau from brain (Cleveland et al., 1977), and we have confirmed this for individual tau isoforms and constructs (e.g., Fig. 2 *e*). This means that we cannot invoke regular folding patterns such as α-helix or β-sheet to build models of tau. The sedimentation constant of one tau isoform (htau40, 2.6 S) is similar to

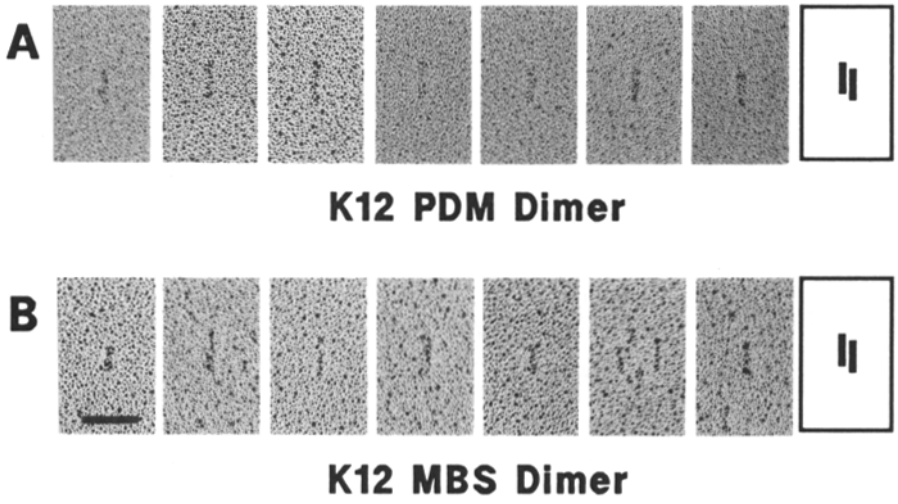

Figure 9. (*A*) K12 dimers crosslinked by PDM (i.e., Cys322 to Cys322); (*B*) K12 dimers crosslinked by MBS (i.e., Cys-322 to nearby Lys). Bar, 50 nm.

that determined by Cleveland et al. (1977) for the tau mixture from brain, confirming that tau must be highly asymmetric even in solution (high axial ratios, cf., Fig. 2 *d*).

These data are consistent with EM. In fact, single tau molecules are remarkably difficult to visualize. They are practically invisible in thin sections of microtubules or in negative stain (Amos, 1977; Herzog and Weber, 1978; Kim et al., 1979). They can be visualized by metal shadowing, but only when very low angles are used (Zingsheim et al., 1979; Hirokawa et al., 1988); in this regard tau is similar to MAP2 (Voter and Erickson, 1982; Gottlieb and Murphy, 1985; Wille et al., 1992*a*,*b*). These data suggest that tau is unusually thin. We have compared the apparent thickness of tau with that of other specimens of known structure, such as single or double stranded DNA or coiled coil α-helical proteins (Wille et al., 1992*a*). We find that tau is more difficult to visualize than these control specimens, suggesting that it has a very low mass per unit length. This is borne out by rough calculations: a rod-like virus such as TMV has 131 kD/nm, a coiled coil α-helical protein (e.g., tropomyosin) has ~1.5

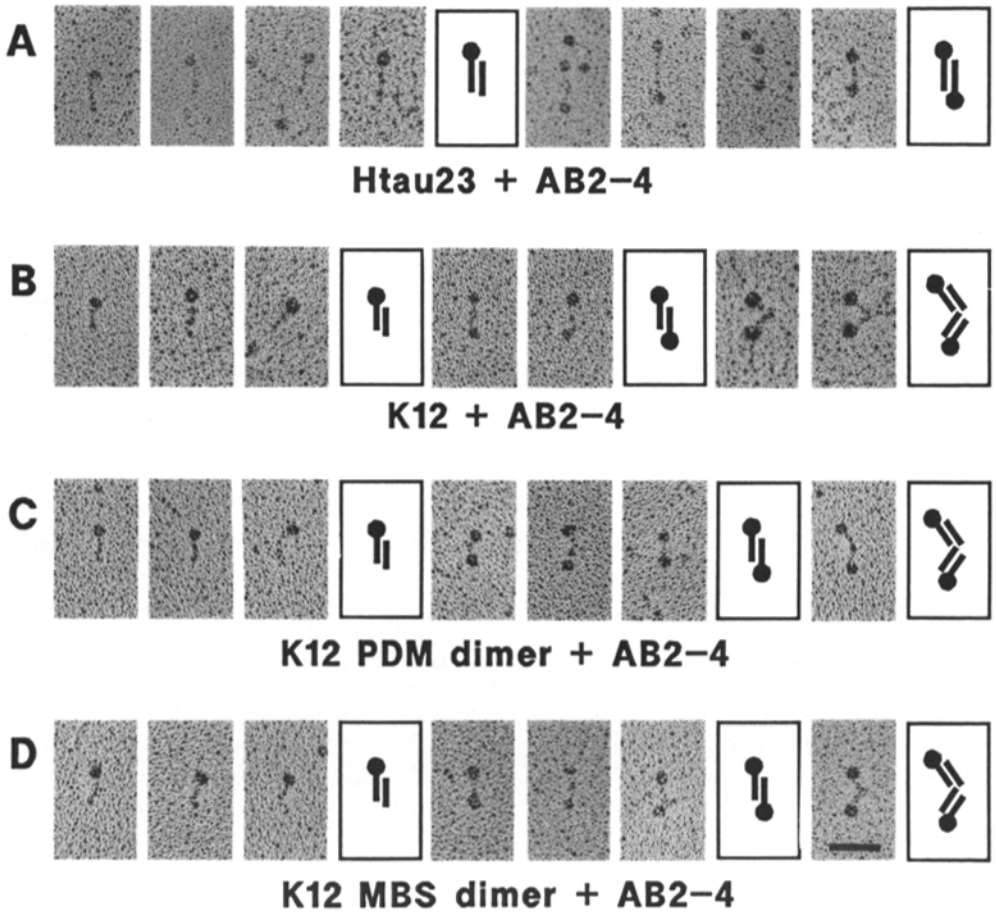

Figure 10. Antibody labeling of htau23, K12, and crosslinked products thereof. (*a*) Htau23 dimers with an antibody at one end (*left*) and with an antibody at each end (*right*) demonstrating the antiparallel dimerization of Htau23; (*b*) K12 dimers with an antibody at one end (*left*), with antibodies at both ends (*middle*) and presumable tetramers with antibodies at the free ends (*right*) indicating that this type of association blocks the epitope; (*c*) K12 dimers crosslinked with PDM, with an antibody at one end (*left*), with antibodies at each end (*middle*) and a tetramer with antibodies at the free ends (*right*); (*d*) K12 dimers crosslinked by MBS with an antibody at one end (*left*), with antibodies at each end (*middle*) and a tetramer with antibodies at the free ends (*right*). Bar, 50 nm.

kD/nm, and B-DNA has ~1.8 kD/nm. By comparison, htau23 has only 1.1 kD/nm. This value is so low that much of tau might simply have the structure of a fairly extended polypeptide chain, stabilized perhaps by a few salt bridges. This in turn would be consistent with other properties such as the resistance to boiling. Not surprisingly, the protein would also not have enough contrast for negative stain EM.

We have compared a variety of tau isoforms and constructs that differ in their NH_2-terminal domains, number of repeats, and COOH-terminal tail. Roughly speaking, the results can be summarized as follows. The overall length depends largely on the region of repeats, whereas the NH_2-terminal domain plus COOH-terminal tail have a smaller contribution. We estimate that the repeat region contributes ~22–25 nm to the overall length, while the regions outside the repeats amount to ~5–10 nm. Thus, K12 is ~25-nm long, htau23 ~35 nm. It is interesting to note that even MAP2, in spite of its more than five times larger mass, is only 2.5 times longer than tau (Gottlieb and Murphy, 1985; Wille et al., 1992*a*).

A notable feature is that constructs differing in only one of the repeats (no. 2) have similar lengths (e.g., K11 and K12, T7R, and T8R, see Fig. 1 and Table I). This suggests that repeat no. 2 is neutral with respect to the overall length. It also means that the repeat region can be regarded as a unit of length. We do not know at present what mode of folding accounts for this property, but we note several constraints for possible models: firstly, the antibody binding site (at the end of the last repeat, Dingus et al., 1991) must be near an end of the rod. Secondly, since dimers are antiparallel and have a similar length as monomers, the cysteine in repeat 3 must be roughly centered in the molecule. In this position it could form a disulfide bond either with repeat 2 (if present), or with a neighboring molecule. In fact, titrations of the SH groups indicate that constructs with four repeats (and thus two internal Cys) have mostly intrachain disulfide bonds, whereas constructs with only three repeats contain disulfide bonds only in the aggregated state (dimers and higher, unpublished data).

One problem in the structure analysis of tau is that the protein is heterogeneous when isolated from brain tissue; it contains several isoforms, each of which can be in different states of phosphorylation which in turn affects its structural properties (Hagestedt et al., 1989). In particular the protein tends to associate into fiber-like aggregates of various extent and order which we have studied in the past, but these studies have not revealed the structure of single tau isoforms. This prompted us to investigate recombinant tau protein because it allowed us to avoid the heterogeneity and phosphorylation of the protein. The lengths we observe for the Tau isoforms are generally less than the 56 nm reported by Hirokawa et al. (1988). We find this value only with contructs having artificially duplicated repeat domains (see Table I). It is difficult to trace the origin of the discrepancy because these authors used a different method of sample preparation and the heterogeneous protein from brain, but it is conceivable that oligomerization plays a role. A similar argument probably holds for the lengths of tau subunits in fibrous structures described in our previous studies (Hagestedt et al., 1989).

Synthetic Paired Helical Filaments and Relationship with Alzheimer PHFs

A particularly intriguing aspect of this work is the finding that constructs K11 and K12 are capable of forming synthetic paired helical filaments. They resemble the natural ones found in Alzheimer neurofibrillary tangles in most respects, such as periodicity, diameter, and the appearance of a pair of twisted filaments. In the case of Alzheimer PHFs one distinguishes a fuzzy coat which can be removed by pronase, and the pronase-resistant core. The latter contains the repeat region of tau while the NH_2-terminal domain and the COOH-terminal tail can be digested away (Goedert et al., 1988; Ksiezak-Reding et al., 1991; Jakes et al., 1991). Thus the core of Alzheimer PHFs shares important assembly properties with the constructs that form the paired helical filaments in vitro (compare Figs. 3–5). More specifically, there is a striking similarity between the filaments in vitro and the "soluble" PHF preparation (prepared after Greenberg and Davies, 1990). This includes the presence of straight filaments (see Crowther, 1991) and short rodlike particles (see Goedert et al., 1992). The straight filaments probably represent a slightly different pathway of selfassembly (leading to polymorphism), whereas short particles may result from breakage of longer filaments.

So far we have obtained the PHF-like filaments only in certain conditions, e.g., acidic pH (5.0–5.5), and only with constructs that consist essentially of the repeat domain (e.g., K11, K12). Full-length tau, such as htau23, did not form PHF-like filaments under similar or other conditions. Moreover, it is known that Alzheimer PHFs are made of abnormally phosphorylated tau (Grundke-Iqbal et al., 1986) whereas there is no phosphorylation in our in vitro experiments. Our current assumption is that the abnormal phosphorylation induces a conformation of tau which is conducive to PHF formation and perhaps causes dissociation from microtubules as well. One may therefore speculate that normal tau has regulatory sequences outside the repeats which normally prevent aggregation into PHFs but whose phosphorylation leads to an Alzheimer-like conformation, whereas K12 can assume that conformation by itself without involving other parts of the tau sequence. Consistent with this, all of the phosphorylation sites of tau reported so far lie outside the repeat region and are not present in K11 or K12 (Ser 416, Steiner et al., 1990; Ser 396, Lee et al., 1991; Ser 199 and 202, Biernat et al., 1992; numbering of htau40). In this context it is interesting to note that monomers as well as dimers of K12 bind to microtubules with similar affinities (unpublished data), so that the microtubule-binding capability is not destroyed by dimerization.

PHF-like filaments can be assembled not only from monomers of the repeat constructs, but also from chemically crosslinked dimers. This raises the possibility that the formation of an antiparallel dimer might precede the incorporation into filaments, i.e.:

repeat domain: monomer → dimer → PHF.

This in turn would suggest that the core of Alzheimer PHFs might consist of antiparallel dimers of repeat domains. On the other hand, full length tau allows the formation of dimers, but normally not of PHFs, so that the second step would be interrupted:

normal tau: monomer → dimer → ?.

Phosphorylation might regulate one or both of these steps and open up the pathological pathway of PHF assembly.

We thank A. Malchert and U. Böning for excellent technical assistance with the cloning, expression, and purification of the tau proteins. We are grateful to Dr. B. Lichtenberg-Kraag (Hamburg) for the data on Alzheimer PHFs, to M. Kniel (Hamburg) for the data on K12 PDM dimer PHFs, to Drs. J. Dingus and R. Vallee (Worcester Foundation) for the gift of the antibody 2-4, Dr. M. Goedert (MRC, Cambridge) and Dr. M. Kirschner (University of California, San Francisco, CA) for the clones of the human or bovine tau, resp., Dr. F. Studier (Brookhaven National Laboratory, Upton, NY) for the pET vectors, and to Drs. A. Pingoud and C. Urbanke (University of Hannover, Germany) for help with ultracentrifuge and CD experiments.

This project was supported by grants of the Bundesministerium für Forschung und Technologie and the Deutsche Forschungsgemeinschaft. This study contains part of the doctoral thesis of H. Wille.

Received for publication 18 February 1992 and in revised form 24 April 1992.

References

Amos, L. A. 1977. Arrangement of high molecular weight associated proteins on purified mammalian brain microtubules. *J. Cell Biol.* 762:642–654.

Baudier, J., and R. D. Cole. 1987. Phosphorylation of tau proteins to a state like that in Alzheimer's brain is catalyzed by a calcium/calmodulin dependent kinase and modulated by phospholipids. *J. Biol. Chem.* 262:17577–17583.

Biernat, J., E.-M. Mandelkow, C. Schröter, B. Lichtenberg-Kraag, B. Steiner, B. Berling, H. E. Meyer, M. Mercken, A. Vandermeeren, M. Goedert, and E. Mandelkow. 1992. The switch of tau protein to an Alzheimer-like state includes the phosphorylation of two serine-proline motifs upstream of the microtubule binding region. *EMBO (Eur. Mol. Biol. Organ.) J.* 11:1593–1597.

Cantor, C. R., and R. P. Schimmel. 1980. Biophysical Chemistry, Part II: Techniques for the Study of Biological Structure and Function. Freeman and Co., San Francisco. 557–562.

Cleveland, D. W., S.-Y. Hwo, and M. W. Kirschner. 1977. Physical and chemical properties of purified tau factor and the role of tau in microtubule assembly. *J. Mol. Biol.* 116:227–247.

Crowther, R. A., and C. M. Wischik. 1985. Image reconstruction of the Alzheimer paired helical filament. *EMBO (Eur. Mol. Biol. Organ.) J.* 4:3661–3665.

Crowther, R. A. 1991. Straight and paired helical filaments in Alzheimer disease have a common structural unit. *Proc. Natl. Acad. Sci. USA.* 88:2288–2292.

Dingus, J., R. Obar, J. Hyams, M. Goedert, and R. B. Vallee. 1991. Use of a heat-stable MAPs class-specific antibody to investigate the mechanism of microtubule binding. *J. Biol. Chem.* 266:18854–18860.

Drewes, G., B. Lichtenberg-Kraag, F. Döring, E.-M. Mandelkow, J. Biernat, J. Goris, M. Doree, E. Mandelkow. 1992. Mitogen-activated protein (MAP) kinase transforms tau protein into an Alzheimer-like state. *EMBO (Eur. Mol. Biol. Organ.) J.* 6:2131–2138.

Drubin, D., and M. Kirschner. 1986. Tau protein function in living cells. *J. Cell Biol.* 103:2739–2746.

Goedert, M., C. Wischik, R. Crowther, J. Walker, and A. Klug. 1988. Cloning and sequencing of the cDNA encoding a core protein of the paired helical filament of Alzheimer disease: identification as the microtubule-associated protein tau. *Proc. Natl. Acad. Sci. USA.* 85:4051–4055.

Goedert, M., M. Spillantini, R. Jakes, D. Rutherford, and R. A. Crowther. 1989. Multiple isoforms of human microtubule-associated protein-tau: sequences and localization in neurofibrillary tangles of Alzheimers-disease. *Neuron.* 3:519–526.

Goedert, M., S. S. Sisodia, and D. L. Price. 1991. Neurofibrillary tangles and β-amyloid deposits in Alzheimer's disease. *Curr. Opin. Neurobiol.* 1:441–447.

Goedert, M., G. Spillantini, N. J. Cairns, and R. A. Crowther. 1992. Tau proteins of Alzheimer paired helical filaments: abnormal phosphorylation of all six brain isoforms. *Neuron.* 8:159–168.

Gottlieb, R. A., and D. B. Murphy. 1985. Analysis of the microtubule-binding domain of MAP-2. *J. Cell Biol.* 101:1782–1789.

Greenberg, S. G., and P. Davies. 1990. A preparation of Alzheimer paired helical filaments that displays distinct tau-proteins by polyacrylamide-gel electrophoresis. *Proc. Natl. Acad. Sci. USA.* 87:5827–5831.

Grundke-Iqbal, I., K. Iqbal, Y. Tung, M. Quinlan, H. Wisniewski, and L. Binder. 1986. Abnormal phosphorylation of the microtubule-associated protein tau in Alzheimer cytoskeletal pathology. *Proc. Natl. Acad. Sci. USA.* 83:4913–4917.

Hagestedt, T., B. Lichtenberg, H. Wille, E.-M. Mandelkow, and E. Mandelkow. 1989. Tau protein becomes long and stiff upon phosphorylation: correlation between paracrystalline structure and degree of phosphorylation. *J. Cell Biol.* 109:1643–1651.

Herzog, W., and K. Weber. 1978. Fractionation of brain microtubule-associated proteins. Isolation of two different proteins which stimulate tubulin polymerisation in vitro. *Eur. J. Biochem.* 92:1–8.

Himmler, A., D. Drechsel, M. Kirschner, and D. Martin. 1989. Tau consists of a set of proteins with repeated C-terminal microtubule-binding domains and variable N-terminal domains. *Mol. Cell. Biol.* 9:1381–1388.

Hirokawa, N., Y. Shiomura, and S. Okabe. 1988. Tau proteins: the molecular structure and mode of binding to microtubules. *J. Cell Biol.* 107:1449–1459.

Jakes, R., M. Novak, M. Davison, and C. M. Wischik. 1991. Identification of 3- and 4-repeat tau isoforms within the PHF in Alzheimer's disease. *EMBO (Eur. Mol. Biol. Organ.) J.* 10:2725–2729.

Kim, H., L. I. Binder, and J. L. Rosenbaum. 1979. The periodic association of MAP2 with brain microtubules in vitro. *J. Cell Biol.* 80:266–276.

Kondo, J., T. Honda, H. Mori, Y. Hamada, R, Miura, M. Ogawara, and Y. Ihara. 1988. The carboxyl third of tau is tightly bound to paired helical filaments. *Neuron.* 1:827–834.

Kosik, K. 1990. Tau protein and Alzheimer's disease. *Curr. Opin. Cell Biol.* 2:101–104.

Ksiezak-Reding, H., and S. H. Yen. 1991. Structural stability of paired helical filaments requires microtubule-binding domains of tau: a model for self-association. *Neuron.* 6:717–728.

Laemmli, U. K. 1970. Cleavage of structural proteins during the assembly of the head of bacteriophage T4. *Nature (Lond.).* 227:680–685.

Lee, G., N. Cowan, and M. Kirschner. 1988. The primary structure and heterogeneity of tau protein from mouse brain. *Science (Wash. DC).* 239:285–288.

Lee, V. M. Y., B. J. Balin, L. Otvos, and J. Q. Trojanowski. 1991. A68 - a major subunit of paired helical filaments and derivatized forms of normal tau. *Science (Wash.).* 251:675–678.

Lichtenberg-Kraag, B., E.-M. Mandelkow, J. Biernat, B. Steiner, C. Schröter, N. Gustke, H. Meyer, and E. Mandelkow. 1992. Phosphorylation dependent interaction of neurofilament antibodies with tau protein: Epitopes, phosphorylation sites, and relationship with Alzheimer tau. *Proc. Natl. Acad. Sci. USA.* In press.

Lichtenberg-Kraag, B., and E.-M. Mandelkow. 1990. Isoforms of tau protein from mammalian brain and avian erythrocytes: structure, self-assembly, and elasticity. *J. Struct. Biol.* 105:46–53.

Montejo de Garcini, E., and J. Avila. 1987. In vitro conditions for the self-polymerization of the microtubule-associated protein, tau factor. *J. Biochem.* 102:1415–1421.

Sambrook, J., E. F. Frisch, and T. Maniatis. 1989. Molecular Cloning: A Laboratory Manual. Cold Spring Harbor Laboratory Press, Cold Spring Harbor, NY. Part I, 1.1–7.87.

Steiner, B., E.-M. Mandelkow, J. Biernat, N. Gustke, H. E. Meyer, B. Schmidt, G. Mieskes, H. D. Söling, D. Drechsel, M. W. Kirschner, M. Goedert, and E. Mandelkow. 1990. Phosphorylation of microtubule-associated protein tau: identification of the site for Ca^{++} -calmodulin dependent kinase and relationship with tau phosphorylation in Alzheimer tangles. *EMBO (Eur. Mol. Biol. Organ.) J.* 9:3539–3544.

Studier, W. F., A. H. Rosenberg, J. J. Dunn, and J. W. Dubendorff. 1990. Use of T7 RNA polymerase to direct the expression of cloned genes. *Methods Enzymol.* 185:60–89.

Tucker, R. P. 1990. The roles of microtubule-associated proteins in brain morphogenesis: a review. *Brain Res. Rev.* 15:101–120.

Tyler, J. M., and D. Branton. 1980. Rotary shadowing of extended molecules dried from glycerol. *J. Ultrastruct. Res.* 71:95–102.

Van Bruggen, E., J. van Breemen, W. Keegstra, E. Bockema, and M. van Heel. 1986. Two-dimensional crystallization experiments. *J. Microsc.* 141:11–20.

Voter, W. A., and H. P. Erickson. 1982. Electron microscopy of MAP2 (Microtubule-associated protein 2). *J. Ultrastruct. Res.* 80:374–382.

Wiche, G., C. Oberkanins, and A. Himmler. 1990. Molecular structure and function of microtubule-associated proteins. *Int. Rev. Cytol.* 124:217–273.

Wille, H., E.-M. Mandelkow, J. Dingus, R. Vallee, L. Binder, and E. Mandelkow. 1992*a*. Domain structure and antiparallel dimers of microtubule-associated protein 2 (MAP2). *J. Struct. Biol.* 108:49–61.

Wille, H., E.-M. Mandelkow, and E. Mandelkow. 1992*b*. The juvenile microtubule-associated protein MAP2c is a rod-like molecule that forms antiparallel dimers. *J. Biol. Chem.* 267:10737–10742.

Wischik, C., R. Crowther, M. Stewart, and M. Roth. 1985. Subunit structure of paired helical filaments in Alzheimer's disease. *J. Cell Biol.* 100:1905–1912.

Zingsheim, H.-P., W. Herzog, and K. Weber. 1979. Differences in surface morphology of microtubules reconstituted from pure brain tubulin using two different microtubule-associated proteins: the high molecular weight MAP2 proteins and tau proteins. *Eur. J. Cell. Biol.* 19:175–183.